Changes in Inorganic Fine Particulate Matter Sensitivities to Precursors Due to Large-Scale US Emissions Reductions *

Jareth Holt, Noelle E. Selin and Susan Solomon

The MIT Joint Program on the Science and Policy of Global Change combines cutting-edge scientific research with independent policy analysis to provide a solid foundation for the public and private decisions needed to mitigate and adapt to unavoidable global environmental changes. Being data-driven, the Program uses extensive Earth system and economic data and models to produce quantitative analysis and predictions of the risks of climate change and the challenges of limiting human influence on the environment—essential knowledge for the international dialogue toward a global response to climate change.

To this end, the Program brings together an interdisciplinary group from two established MIT research centers: the Center for Global Change Science (CGCS) and the Center for Energy and Environmental Policy Research (CEEPR). These two centers—along with collaborators from the Marine Biology Laboratory (MBL) at Woods Hole and short- and long-term visitors—provide the united vision needed to solve global challenges.

At the heart of much of the Program's work lies MIT's Integrated Global System Model. Through this integrated model, the Program seeks to: discover new interactions among natural and human climate system components; objectively assess uncertainty in economic and climate projections; critically and quantitatively analyze environmental management and policy proposals; understand complex connections among the many forces that will shape our future; and improve methods to model, monitor and verify greenhouse gas emissions and climatic impacts.

This reprint is one of a series intended to communicate research results and improve public understanding of global environment and energy challenges, thereby contributing to informed debate about climate change and the economic and social implications of policy alternatives.

Ronald G. Prinn and John M. Reilly,
Program Co-Directors

For more information, contact the Program office:
MIT Joint Program on the Science and Policy of Global Change

Postal Address:
Massachusetts Institute of Technology
77 Massachusetts Avenue, E19-411
Cambridge, MA 02139 (USA)

Location:
Building E19, Room 411
400 Main Street, Cambridge

Access:
Tel: (617) 253-7492
Fax: (617) 253-9845
Email: ***globalchange@mit.edu***
Website: ***http://globalchange.mit.edu/***

Changes in Inorganic Fine Particulate Matter Sensitivities to Precursors Due to Large-Scale US Emissions Reductions

Jareth Holt,*,[†] Noelle E. Selin,[†,‡] and Susan Solomon[†]

[†]Department of Earth, Atmospheric and Planetary Sciences, Massachusetts Institute of Technology, 77 Massachusetts Avenue, Building 54-1711, Cambridge, Massachusetts 02139, United States

[‡]Engineering Systems Division, Massachusetts Institute of Technology, Cambridge, Massachusetts 02139, United States

S *Supporting Information*

ABSTRACT: We examined the impact of large US emissions changes, similar to those estimated to have occurred between 2005 and 2012 (high and low emissions cases, respectively), on inorganic $PM_{2.5}$ sensitivities to further NO_x, SO_2, and NH_3 emissions reductions using the chemical transport model GEOS-Chem. Sensitivities to SO_2 emissions are larger year-round and across the US in the low emissions case than the high emissions case due to more aqueous-phase SO_2 oxidation. Sensitivities to winter NO_x emissions are larger in the low emissions case, more than 2× those of the high emissions case in parts of the northern Midwest. Sensitivities to NH_3 emissions are smaller (~40%) in the low emissions case, year-round, and across the US. Differences in NO_x and NH_3 sensitivities indicate an altered atmospheric acidity. Larger sensitivities to SO_2 and NO_x in the low emissions case imply that reducing these emissions may improve air quality more now than they would have in 2005; conversely, NH_3 reductions may not improve air quality as much as previously assumed.
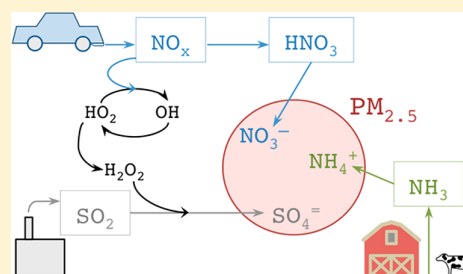
INTRODUCTION

Fine particulate matter ($PM_{2.5}$) adversely affects cardiovascular and respiratory functioning[1] and is a key focus of air quality policies such as the National Ambient Air Quality Standards (NAAQS). Designing effective policies requires knowledge of how $PM_{2.5}$ responds to changes in its precursors—its sensitivity to emissions. The precursors of inorganic $PM_{2.5}$ are nitrogen oxides (NO_x), sulfur dioxide (SO_2), and ammonia (NH_3). US NO_x and SO_2 emissions decreased by 42% and 62%, respectively, between 2005 and 2012, while NH_3 emissions remained approximately constant.[2] These emissions changes are potentially large enough to change the sensitivity of $PM_{2.5}$ to future emissions reductions and hence change the expected benefits of air quality policies. We analyze where and to what extent large changes in precursor emissions, similar to those that occurred between 2005 and 2012, alter US $PM_{2.5}$ sensitivities to further emissions reductions.

Several chemical mechanisms affect $PM_{2.5}$ concentrations. Nitric acid (HNO_3) is formed from NO_x, and the fraction of NH_3 and HNO_3 in particulates (the partitioning of these species) depends on ambient temperature, humidity, and acidity. NH_3 is the primary basic species, forming ammonium (NH_4^+) in particles to neutralize acidic nitrate (NO_3^-) and sulfate (SO_4^{2-}, formed from SO_2). $PM_{2.5}$ sensitivities to NH_3 emissions are large, and it has been argued that reducing NH_3 is a cost-effective strategy to reduce $PM_{2.5}$.[3−8] Sulfate is not volatile like NH_3 and HNO_3, but it influences the ambient acidity. $PM_{2.5}$ concentrations can even increase as SO_4^{2-} concentrations decrease, by allowing more HNO_3 to condense.[3,9] However, multiple reactions oxidize SO_2 into SO_4^{2-}, and each reaction responds differently to NO_x and hydrocarbon concentrations.[10,11]

$PM_{2.5}$ sensitivities have been estimated using a variety of approaches, including finite differences,[12,13] direct decomposition,[14−17] and adjoint modeling.[18,19] Sensitivity estimates calculate derivatives based around atmospheric conditions associated with particular emissions. Extrapolating these estimates to other levels of emissions is associated with some degree of error. Zhang et al.[17] show that a linear extrapolation underestimates the $PM_{2.5}$ response to a 50% decrease in NO_x emissions by 15%, averaged over the US, with local underestimates up to 50%. Higher-order sensitivity analysis can more accurately predict responses beyond the linear range,[14] but these approaches are computationally demanding.

Studies of health and economic impacts of emissions often apply estimates of $PM_{2.5}$ sensitivities to parametrize how air quality responds to emissions. Muller and co-workers[12,20,21] use the integrated assessment model APEEP to calculate marginal damages (in US dollars per ton) by increasing emissions from one source by one ton and tracing impacts on human health, agriculture, and other vulnerable structures. The base case in APEEP uses the EPA's 2002 National Emissions Inventory (NEI02), but Muller[21] implements the 2005 inventory

(NEI05). Fann, Baker, and Fulcher[22,23] use the CAMx Particle Source Apportionment Technology to attribute $PM_{2.5}$ concentrations to emissions from each economic sector. Their simulations use NEI05 and projections for 2016 based on proposed air quality rules. Similarly, Fann, Fulcher, and Hubbell[24] use NEI02 with projections for 2015 as the emissions inventory for EPA's Response Surface Model of air quality.[25] In these studies, the projections based on then-proposed rules exhibit 30% decreases in national NO_x and SO_2 emissions between 2001 and 2010.[25] These emissions actually decreased by 34% and 53%, respectively, and NH_3 emissions increased by 17%. Whether sensitivities calculated using older (2002 and 2005) emissions, or even past estimates of current emissions, are sufficiently accurate for health and economic impact assessment depends on the nonlinear response of $PM_{2.5}$.

We evaluate the influence of large NO_x and SO_2 emissions changes (comparable to those that occurred in the US between 2005 and 2012) on $PM_{2.5}$ sensitivities and identify the most important nonlinear processes. We find that lower NO_x emissions lead to higher SO_2 sensitivities across the US and to higher NO_x sensitivities in winter in cold, humid regions such as the northern Midwest. Lower NO_x and SO_2 emissions also yield smaller sensitivities to NH_3. Our results suggest that the benefits of NO_x reductions could be much larger now that emissions are lower, especially in winter (when NH_3 emissions were thought to be dominant). We also show that SO_2 controls are still effective, despite >60% reductions nationally. The potential changes identified highlight the need to review the sensitivities used in health, economic, and policy studies and consider a multipollutant approach to air quality policy.

■ METHODOLOGY

Chemical Transport Model. We use the GEOS-Chem chemical transport model v9-02[26,27] (http://geos-chem.org/). GEOS-Chem has previously been evaluated against measurements of ozone and hydrocarbon concentrations[26] and inorganic $PM_{2.5}$ component concentrations.[7,28,29] It has been used to study US air quality[7,8] and climate change impacts on $PM_{2.5}$ formation.[30−32]

GEOS-Chem simulates ozone-NO_x-hydrocarbon-aerosol chemistry[27] coupled to inorganic aerosol thermodynamics, which determines the partitioning of NH_3 and HNO_3. The thermodynamic module is ISORROPIA II,[33] incorporated into GEOS-Chem by Pye et al.[30] We use nested-grid simulations[34,35] with at $0.5° × 0.67°$ resolution (55 km × 57 km at 40° N) over North America (10°−70° N, 140°−40° W) and $2° × 2.5°$ resolution (222 km × 213 km) elsewhere. The chemical mechanism has a temporal resolution of 20 min and a vertical grid of 47 layers extending to 80 km, with 30 layers in the lowest 11 km and 14 layers in the lowest 2 km. Our simulations are driven by GEOS5 meteorology from the NASA Global Modeling and Assimilation Office (GMAO). Each simulation uses meteorology for January or July of 2005, representing winter and summer conditions.

GEOS-Chem v9-02 has three new features relevant to our simulations. First, it includes soil NO_x emissions that respond dynamically to meteorology and nitrogen deposition.[36] Second, it limits planetary boundary heights from falling lower than a friction velocity-based minimum. This corrects abnormally low nighttime boundary layers in GEOS5 meteorology compared to observations[37] and improves the diurnal variability in simulated chemistry.[28] Third, it reduces the rate of production of NO_3^- from N_2O_5 hydrolysis, reducing some of the high nitrate bias

seen in GEOS-Chem.[28,38,39] These features improve simulated NO_x concentrations (especially the daytime-nighttime difference) and reduce the high NO_3^- bias noted previously.[28,29,38]

Emissions. We use anthropogenic emissions from the EDGAR and RETRO global inventories plus several regional inventories (over e.g., China, Europe).[40] The US inventory is EPA's National Emissions Inventory for 2005 (NEI05). NEI05 provides emissions of NO_x, SO_2, NH_3, several hydrocarbon species, and primary PM. We seasonally adjust NH_3 emissions from NEI05 following Zhang et al.,[38] decreasing winter emissions to better match observations, consistent with process-based inventories.[41]

We created two groups of simulations, based around a high and low emissions case, to test the influence of large-scale emissions reductions on $PM_{2.5}$ sensitivity. The national, annual total emissions of NO_x, SO_2, and NH_3 as reported to the US EPA for 2005 and 2012[2] exhibit a 42% decrease in NO_x, a 62% decrease in SO_2, and a 1% increase in NH_3 emissions. We used these ratios to scale the high emissions case (using NEI05) to the low emissions case. Table 1 shows the resulting total

Table 1. Anthropogenic Emissions (in kilotonnes = 10^6 kg) of Inorganic $PM_{2.5}$ Precursor Emissions over the North American Domain in the Base Simulations of Each Case (High and Low Emissions) and the Changes in Emissions ΔE for Sensitivity Calculations

	E (high)		E (low)		ΔE	
	Jan	Jul	Jan	Jul	Jan	Jul
NO_x	1343.3	1248.9	909.6	855.3	206.5	187.5
SO_2	849.4	834.2	491.0	484.5	115.6	112.8
NH_3	169.9	548.6	170.7	552.3	15.9	73.8

anthropogenic emissions over the nested-grid domain. CO, VOC, and primary $PM_{2.5}$ emissions in the US also changed by −16%, +1%, and +12% between 2005 and 2012. Primary $PM_{2.5}$ emissions have a direct effect on total $PM_{2.5}$ levels, so sensitivities to primary emissions stay constant. Changes to VOC and CO emissions would have effects on both organic and inorganic $PM_{2.5}$ components. Since organic $PM_{2.5}$ is not included in our study, we did not change VOC or CO emissions, but we do discuss the potential oxidative impact of CO emissions changes.

While our scaling approach matches changes in total emissions, the spatial pattern of sources may have changed as well. Reported NO_2 column densities over major cities in the US are between 24% and 48% lower in 2012 than in 2005,[42] but NO_2 concentrations in the four quadrants of the US are ∼37−40% lower in 2011 than in 2005.[43] Russell, Valin, and Cohen[44] estimate that NO_x emissions from major power plants decreased by 26% between 2005 and 2011, while mobile emissions decreased by 34%. Fioletov et al.[45] find that SO_2 concentrations over major US power plants are consistently ∼40% lower in 2008−2010 than in 2005−2007. This previous work suggests that the total emissions decreases are distributed broadly across the country and across sectors. Hence, our scaling approach approximates the actual emissions changes.

We calculate $PM_{2.5}$ sensitivities as the finite difference in $PM_{2.5}$ concentrations between simulations with emissions slightly increased and decreased around the baseline. Specifically, sensitivity is computed as

$$S(c) = \frac{PM_{2.5}(E(c) + \Delta E) - PM_{2.5}(E(c) + \Delta E)}{2 \times \Delta E} \qquad (1)$$

where c is the case (high or low emissions) with national-total emissions mass $E(c)$; ΔE is the mass change in emissions; and $PM_{2.5}(E)$ is the $PM_{2.5}$ concentration in the simulation with emissions E. Emissions of other species are fixed at their baseline values for that case. The resulting sensitivities have units of ng m^{-3} kt^{-1}, where kt denotes 1000 t of emissions. The mass changes in emissions for each species and each season are in Table 1.

Calculating sensitivities using mass changes helps clarify the mechanisms that contribute most to sensitivity changes. Since $PM_{2.5}$ is the aggregate of multiple species, normalized (%-based) sensitivities can change between the emissions cases even if oxidation, deposition, and transport processes remain constant. We also use a centered finite difference, as opposed to a one-sided difference that may be more reflective of the effects of a regulation (i.e., a decrease in emissions). This allows our results to be comparable to the adjoint and direct decoupled methods of calculating sensitivities, which also produce centered derivatives.

RESULTS

Model Evaluation. We evaluated model performance by comparing inorganic $PM_{2.5}$ component concentrations in our high emissions case (using NEI05 emissions) to measurements in January and July of 2005 from two monitoring networks: the Interagency Monitoring of Protected Visual Environments (IMPROVE) network[46] and the EPA Air Quality System (AQS[47]). Here we report the coefficient of determination (squared correlation, r^2) and the normalized mean bias (NMB, model mean over observed mean minus one). The statistics use measured and modeled concentrations paired in both space and time. A more detailed evaluation is provided in the SI (Tables S1 and S2 and Figures S3 and S4).

Our simulation correlates reasonably well ($r^2 > 30\%$) with several measurements: January IMPROVE measurements of all species; both IMPROVE and AQS measurements of July SO_4^{2-}; and January AQS measurements of NH_4^+. Modeled SO_4^{2-} is unbiased in January (NMB < 5%) but slightly low in July (NMB ~ −15%) compared to either set of measurements. Modeled January NH_4^+ and NO_3^- concentrations are biased high (NMB = 86%, 89% respectively, compared to AQS; NMB = 51%, 134% compared to IMPROVE) consistent with previous GEOS-Chem analyses.[28,29,38]

Simon, Baker, and Phillips[48] compare published performance statistics from a range of chemical transport models (not including GEOS-Chem). They find that modeled SO_4^{2-} is unbiased (NMB < 15%), whereas NO_3^- is biased high in winter (NMB 0% to 50%) and low in summer (−15% to −75%). Squared correlations for SO_4^{2-} and NH_4^+ are between 25% and 60%, compared to 10%−45% for NO_3^-. Comparing their results to our statistics indicates that GEOS-Chem has a higher bias in winter NO_3^- than is typical but otherwise performs similar to other models.

Within the northern Midwest − the same region as used for the thermodynamic analysis in Figure 3 − the NMB of modeled NO_3^- compared to IMPROVE measurements is 109% and $r^2 = 42\%$, showing that GEOS-Chem estimates NO_3^- in this area better than in the national average (NMB = 134%, r^2 = 39%). While sulfate biases are generally smaller than nitrate, modeled SO_4^{2-} is low in this area (NMB = −48%), and a

simple scaling to lower model SO_4^{2-} would bring the NO_3^- NMB down to 97%. Modeled NO_3^- is thus better simulated in the region where its behavior is most important to our analysis, detailed below.

PM2.5 Concentrations. Figure 1 shows the total inorganic $PM_{2.5}$ concentrations from the high and low emissions cases. Figure S1 shows the components individually.
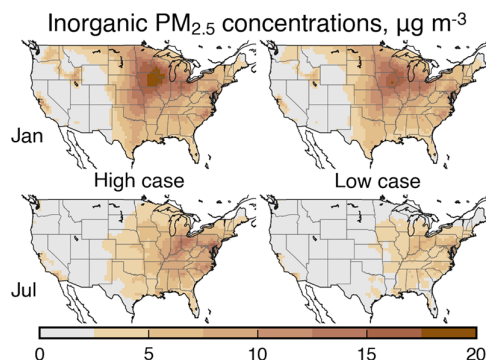

Figure 1. Spatial maps of the modeled surface concentrations of inorganic $PM_{2.5}$. Columns show the high and low emissions cases; rows show January and July averages.

January $PM_{2.5}$ peaks in the northern Midwest and is elevated over the eastern US. Northern Midwest $PM_{2.5}$ is primarily composed of NH_4^+ and NO_3^- with low SO_4^{2-}. National average NO_3^-, NH_4^+, and $PM_{2.5}$ concentrations in the low emissions case are 7.7%, 9.5%, and 11.6% lower than in the high emissions case, respectively. However, these decreases are not uniform across the US. The area around Kentucky, Ohio, and Virginia shows *higher* aerosol NO_3^- in the low emissions case than in the high emissions case. Higher NO_3^- is offset by lower SO_4^{2-}, so total $PM_{2.5}$ concentrations are <0.15 μg m^{-3} higher in the low emissions case than the high emissions case.

Summer $PM_{2.5}$ concentrations are generally lower than in winter but still higher over the eastern US than the western US. The largest mass contribution to summer $PM_{2.5}$ comes from SO_4^{2-}, followed by NH_4^+. SO_4^{2-}, NH_4^+, and total $PM_{2.5}$ are all ~40% lower in the low emissions case than in the high emissions case, compared to 62% lower SO_2 emissions. Some urban and regional areas (San Diego, New Orleans, Atlanta, Houston/Eastern Texas, Philadelphia/New Jersey, North Carolina, Illinois-Indiana-Ohio) show substantial summer aerosol NO_3^- concentrations, up to 5 μg m^{-3}. Aerosol NO_3^- levels in these regions are lower in the low emissions case by 30.5% on average, compared to 42% lower NO_x emissions. However, model-measurement correlations of summer NO_3^- concentrations are small ($r^2 = 0.8\%$, 3.2% compared to IMPROVE and AQS, respectively).

PM2.5 Sensitivity to Emissions. Here we describe the sensitivities of $PM_{2.5}$ to the different precursor emissions, shown in Figure 2 and computed using eq 1.

January $PM_{2.5}$ is most sensitive to NH_3 emissions (Figure 2, top panel, bottom row) in both the high and low emissions cases. Sensitivity to NH_3 peaks in the northern Midwest at values of 118 ng m^{-3} kt^{-1} in the high emissions case. In comparison, maximum winter sensitivities to NO_x and SO_2 are 8 and 10 ng m^{-3} kt^{-1}, respectively. Over the southeastern US and the mid-Atlantic coast, winter sensitivities to SO_2 are prominent and can be >10% of the (local) sensitivity to NH_3.
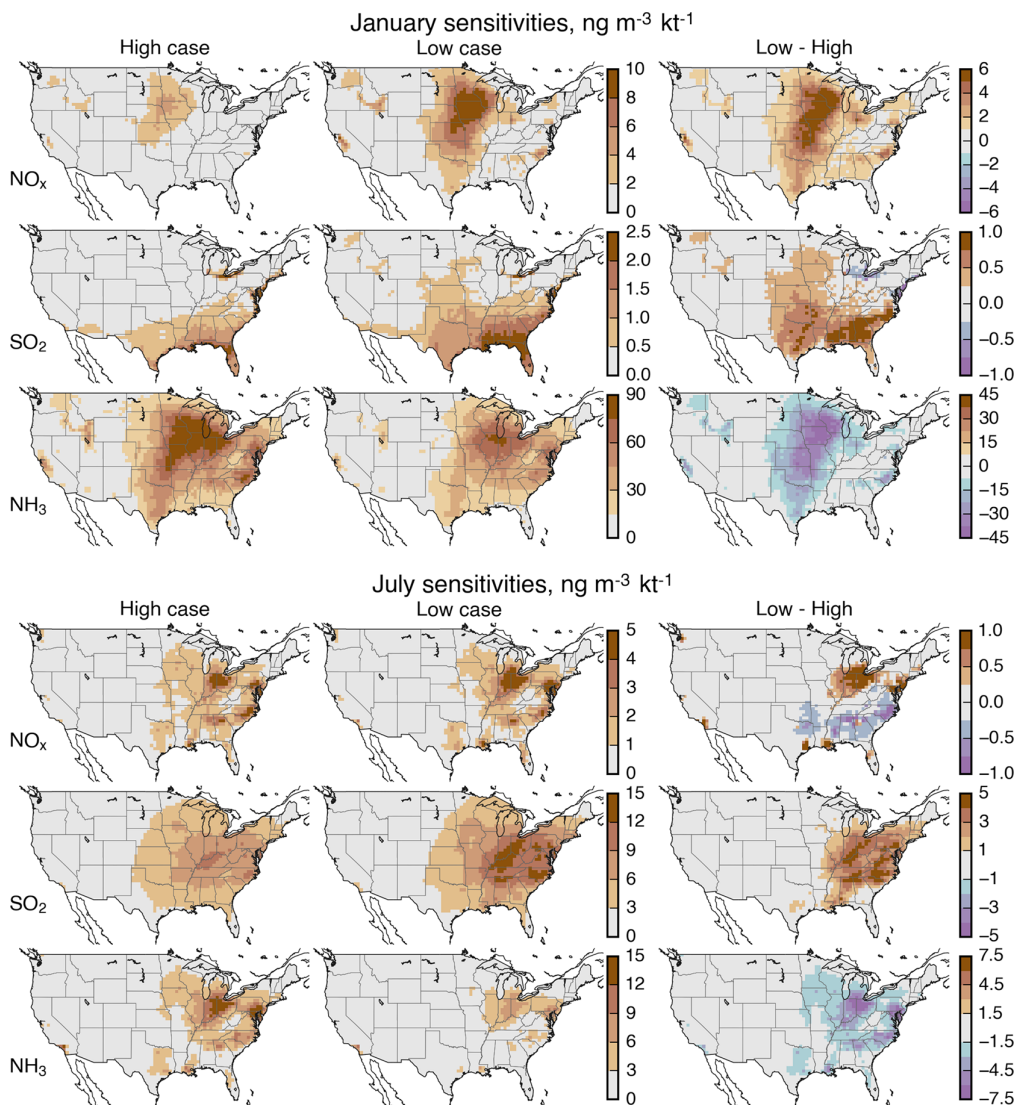
Figure 2. Sensitivities of $PM_{2.5}$ concentrations to emissions of the precursors NO_x, SO_2, and NH_3, in units of ng m^{-3} of $PM_{2.5}$ per thousand metric tons (kt) of emissions. The top and bottom panels show sensitivities in January and July, respectively. The columns show the high emissions case, the low emissions case, and their difference.

We find slight (<0.65 ng m^{-3} kt^{-1}) negative sensitivities to winter SO_2 emissions near the eastern Great Lakes.

The differences in January sensitivities between the high and low emissions cases show two policy-relevant features. First, sensitivities to NH_3 are much smaller in the low emissions case: 28% smaller in the national average and up to 72% smaller in the northern Midwest. In contrast, January sensitivities to NO_x are larger in the low emissions case: 202% larger in the national average. Second, average sensitivities to January SO_2 emissions are 42% larger in the low emissions case. There are some local exceptions, such as the northeast US, that show slightly smaller sensitivities in the low emissions case.

In contrast to January, the July sensitivities to different precursors have similar magnitudes. July $PM_{2.5}$ sensitivities to SO_2 emissions (Figure 2, lower panel, middle row) are high across the eastern US and peak in the Ohio River Valley. Sensitivities to SO_2 are larger in the low emissions case than the

high emissions case at nearly every grid point: 23% larger in the national average and up to 80% larger in the eastern US.

In the high emissions case, summer sensitivities to NH_3 emissions are large around the Great Lakes region, eastern Pennsylvania, and a few urban regions. These regions also have high summer sensitivities to NO_x emissions, though the magnitudes are different: peak summer sensitivities to NH_3 and to NO_x in the Great Lakes region are 18.6 and 4.9 ng m^{-3} kt^{-1}, respectively. Summer sensitivities to NH_3 are 38% smaller on average in the low emissions case than the high emissions case.

Summer sensitivities to NO_x emissions are evident around the Great Lakes and a few localized areas on the Atlantic and Gulf coasts. Unlike NH_3, the sign of changes in sensitivity to summer NO_x emissions varies: the Great Lakes region and some urban areas have larger sensitivities in the low emissions case, whereas the southeastern US has smaller sensitivities. In grid cells where sensitivity to NO_x is larger in the low emissions

case, it is 37% larger on average; in cells where the sensitivity is smaller, it is 29% smaller on average.

■ UNDERLYING PROCESSES

We investigated several processes that could contribute to differences in $PM_{2.5}$ sensitivities between the high and low emissions cases. In this section, we focus on two particularly important aspects. First, the thermodynamics of ammonium nitrate formation determines winter sensitivities throughout the Midwest. Second, the kinetics of SO_2 oxidation help explain changes in sensitivity to both NO_x and SO_2 emissions across the eastern US in both seasons. In the SI, we describe how well a linear model based on the high emissions case sensitivities predicts the $PM_{2.5}$ concentrations in the low emissions case, showing how sensitivity changes impact the performance of a simplified model.

Thermodynamics of Ammonium Nitrate Formation. Cold and humid environments, such as the northern Midwest in winter, promote condensation of NH_3 and HNO_3 into $PM_{2.5}$. NH_4^+ and NO_3^- concentrations are high in this region (Figure S1) as are sensitivities to NH_3 and NO_x emissions (Figure 2). The differences in NO_x and NH_3 sensitivities between the high and low emissions cases are highly correlated ($r^2 = 94\%$) and opposite. In addition, $PM_{2.5}$ concentrations in this region are similar in the high and low emissions cases −18 and 16 $\mu g \ m^{-3}$, respectively.

To focus on thermodynamic effects, we used ISORROPIA II,[33] the thermodynamic module in GEOS-Chem, to explore how $PM_{2.5}$ concentrations vary with total available HNO_3 and NH_3. SO_4^{2-} concentrations, temperature, and relative humidity are fixed at their average values between 89 and 97°W and 39.75 and 45.25°N: 1.27 $\mu g \ m^{-3}$, −8.1 °C, and 83%. Figure 3
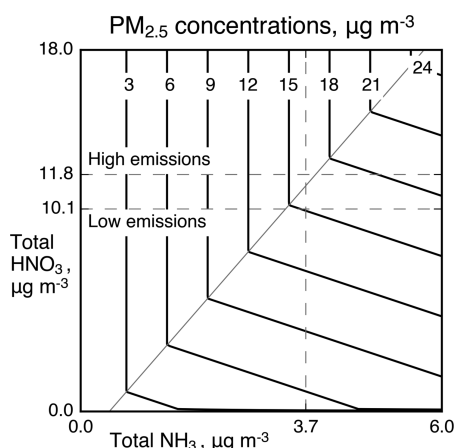
Figure 3. $PM_{2.5}$ concentrations in the thermodynamic model ISORROPIA using temperature, relative humidity, and SO_4^{2-} concentrations typical of the northern Midwest in January. The dashed lines indicate simulated concentrations in the high and low emissions cases. The solid gray line denotes where there is exactly enough NH_3 to neutralize both SO_4^{2-} and NO_3^-.

shows $PM_{2.5}$ under these conditions. There is a line at which the system is neutral with respect to NH_3, i.e. where there is exactly enough NH_3 to fully neutralize both the SO_4^{2-} and NO_3^-, and this neutrality line distinctly separates nitrate-limited and nitrate-saturated regimes. Below the line, $PM_{2.5}$ concentrations depend strongly on HNO_3 concentrations (nitrate-

limited); above the line, $PM_{2.5}$ concentrations depend only on NH_3 concentrations (nitrate-saturated). Also shown are the NH_3 and HNO_3 concentrations from the high and low emissions cases, demonstrating why there is a large change in sensitivity: the high emissions case is nitrate-saturated, so that large changes in emissions yielded little change in $PM_{2.5}$, whereas the low emissions case is nitrate-limited, implying far greater sensitivity to NO_x emissions. A broad area in the northern Midwest presents conditions for which the line between nitrate-limited and nitrate-saturated is sharp, and nitrate limitation occurs to some degree across the US in the winter low emissions case.

Kinetics of SO_2 Oxidation. The oxidation rate of SO_2 into SO_4^{2-} determines whether $PM_{2.5}$ forms before SO_2 is transported or deposited and hence directly affects $PM_{2.5}$ sensitivities to SO_2 emissions. SO_2 oxidation occurs in both gas and aqueous phases.[49] Gas-phase oxidation involves the reaction of SO_2 with hydroxyl radicals (OH). In the aqueous-phase, SO_2 diffuses into cloud droplets, where it reacts with other soluble gases (mostly hydrogen peroxide, H_2O_2) to form SO_4^{2-}. If cloud droplets evaporate instead of precipitate, SO_4^{2-} remains as $PM_{2.5}$. GEOS-Chem outputs the production rate of SO_4^{2-} from the gas-phase reaction and from three additional reactions (aqueous H_2O_2, aqueous O_3, and on sea salt particles) individually, allowing the formation pathway to be explored in detail.

The rate and location of SO_2 oxidation depends on whether the OH or H_2O_2 reaction dominates. NO_x concentrations determine relative concentrations of OH and the hydroperoxy radical HO_2, which reacts with itself to form H_2O_2. Lower NO_x concentrations promote less OH and more H_2O_2, favoring aqueous SO_2 oxidation. More complex organic peroxy radicals can also produce H_2O_2, and their concentrations also increase as NO_x concentrations decrease.

We explored oxidation changes in the high and low emissions cases by examining the fraction of oxidation occurring in the aqueous phase (Figure 4) . The low emissions case has a larger
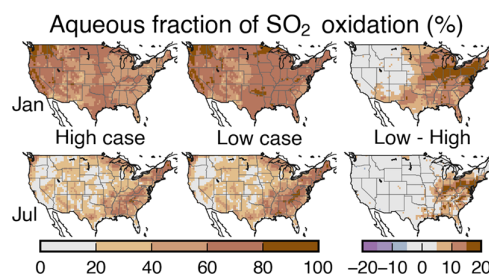
Figure 4. Fraction of SO_2 oxidation that occurs through the aqueous H_2O_2 reaction. This fraction is based on the column oxidation, i.e., the amount of oxidation that occurs throughout the entire atmosphere overlying a grid cell.

fraction of aqueous-phase SO_2 oxidation, as expected from lower NO_x concentrations. In January, the largest differences are in the northern and northeastern US, where aqueous oxidation is 50% of total oxidation in the high emissions case and 70% in the low emissions case. In July, the largest differences are in the Ohio River Valley: 35% aqueous oxidation in the high emissions case and 55% in the low emissions case. In addition, H_2O_2 concentrations in the eastern US (east of 100° W) are 10.6% higher in the low emissions case than in the

high emissions case and OH concentrations are 10.7% lower, supporting the link between NO_x emissions and SO_2 oxidation.

We also investigated whether increased aqueous-phase oxidation would lead to faster SO_2 and SO_4^{2-} rainout due to more sulfur chemistry occurring within cloud droplets. The wet deposition rate (units s^{-1}) is a measure of the speed of rainout (calculation details in the SI). Wet deposition rates are larger in the low emissions case than in the high emissions case by about 5%, compared to 50% larger rates of aqueous SO_2 oxidation. In addition, the differences in $PM_{2.5}$ sensitivities to SO_2 emissions between the high and low emissions cases are spatially correlated (r^2 = 57%) with the fraction of aqueous-phase oxidation. Thus, while faster rainout occurs under low NO_x emissions, it cannot compensate for the increase in aqueous oxidation.

We did not include the 16% decrease in CO emissions between 2005 and 2012 in our simulations. CO reacts with OH to form HO_2 as the counterpart to $NO + HO_2 \rightarrow NO_2 + OH$. Lower CO emissions would lead to a larger OH/HO_2 ratio, less H_2O_2 production, and more gaseous SO_2 oxidation. Thus, lower CO emissions could partially offset the shift to more aqueous-phase SO_2 oxidation in our simulations. However, Duncan et al.[50] suggest that much of the US is now in a NO_x-limited ozone formation regime and hence that NO_x exerts more control on HO_x partitioning (and thus the SO_2 oxidation pathway) than CO does.

■ DISCUSSION

Our study shows large differences in the sensitivities of $PM_{2.5}$ concentrations to precursor emissions between two sets of simulations representing a 2005 baseline (high emissions) and a 2012 analogue (low emissions). We find that winter NO_x reductions represent a potential new opportunity for improving air quality, due to $PM_{2.5}$ being more nitrate-limited under low emissions over much of the US, particularly the Midwest. Lower NO_x emissions also promote aqueous-phase SO_2 oxidation, increasing the sensitivity of $PM_{2.5}$ to SO_2. Sensitivities to NH_3 emissions are lower in the low emissions case, primarily as a direct response to a less acidic atmosphere.

Results for winter in the northern Midwest are driven by the thermodynamic behavior of ammonium nitrate aerosols and are well-constrained for the meteorological conditions (i.e., cold and moist) that prevail there, where concentrations are highest. Figure 3 shows that nitrate availability will play a major role in determining $PM_{2.5}$ in this region in the near future. Accounting for the model's high NO_3^- bias can only push the system further into the nitrate-limited regime. Nevertheless, the large absolute sensitivities to winter NO_x emissions through NO_3^- formation are subject to the model bias. Several studies[28,29,38] have shown that the standard GEOS-Chem simulation overestimates HNO_3 and aerosol NO_3^- concentrations compared to both CASTNet and AQS measurements. There is evidence that certain types of NO_3^- measurements are biased low due to HNO_3 volatilization from filters,[51−53] but adjusting for this does not always provide significant improvement.[54] Studies with other air quality models (notably CAMx[5] and CMAQ[55,56]) have emphasized the potential impact of NH_3 emissions controls on $PM_{2.5}$ concentrations, suggesting that our results are broadly consistent across models.

There are several possible sources of the nitrate bias in GEOS-Chem and other chemical transport models. The dependence of the rate of N_2O_5 hydrolysis on aerosol water, nitrate, chloride, and organic content is uncertain, and nitric

acid concentrations can be highly sensitive to the overall hydrolysis rate.[39,56−58] Hydrolysis within GEOS-Chem includes limitation by nitrate, but this is a topic of ongoing research.[57−61] GEOS-Chem produces more HNO_3 from organic species reactions than other chemical mechanisms at low NO_x concentrations but performs comparably at high NO_x.[62] Heald et al.[29] explore several other potential sources of bias, but no solution has yet been found. However, our thermodynamic analysis increases our confidence that the importance of NO_x emissions to winter $PM_{2.5}$ is not an artifact of this model bias.

Model resolution can also affect model performance. Our simulations have a resolution of ~55 km, compared to the 36 or 12 km resolution typical of regulatory models. Li et al.[63] show differences in GEOS-Chem simulations of US $PM_{2.5}$ at the nested and global resolutions. The maximum values for the three inorganic components are lower at low resolution, but the largest change (29%) is for SO_4^{2-} and changes are most substantial near cities. Thompson, Saari, and Selin[64] show that $PM_{2.5}$ within CAMx changes by 10% across model resolutions from 4 km to 36 km. Punger and West[65] found that CMAQ simulations produce $PM_{2.5}$ mortality estimates 11% higher at 36 km resolution than at 12 km. Much coarser resolutions (>100 km) show lower $PM_{2.5}$ concentrations, but the relative changes are much larger for other components of $PM_{2.5}$ than nitrate, sulfate, and ammonia. Our 55 km resolution is therefore sufficient for studying the regional response of inorganic $PM_{2.5}$ to large, nation-wide changes in emissions, and the computational efficiency of the lower resolution allowed us to explore sensitivities (requiring several simulations for each case).

The change in sensitivity to NH_3 emissions has several implications. First, NH_3 emissions controls have been identified as a potentially cost-effective way to improve air quality.[5] We do not analyze the costs of emissions controls, though the costs of SO_2 and NO_x controls have likely changed from the redistribution of sources, but the impacts of NH_3 emissions controls could be much smaller than previously estimated. Second, previous studies comparing modeled and measured $PM_{2.5}$ in the US[7,29,38,56] have highlighted our generally poor understanding of the magnitude and seasonality of NH_3 emissions. Decreased sensitivity to NH_3 would limit the adverse effects of inaccurate emissions on model performance.

An alternative approach to our sensitivity analysis is to vary emissions based on economic sector (e.g., Caiazzo et al.[13]). However, simultaneous emissions changes in multiple sectors will not have the impact on $PM_{2.5}$ expected from changes in each sector individually. The changes in sensitivities presented here will help identify which sectors could be expected to have strong interactions. For example, broad agricultural NH_3 and NO_x emissions can determine the neutralizing and oxidizing capacity of the background atmosphere and hence the impact of given coal SO_2 emissions on $PM_{2.5}$.

Through this analysis, we find that lower NO_x and SO_2 emissions lead to larger sensitivity to SO_2; smaller sensitivity to NH_3; and larger sensitivity to winter NO_x emissions in the US. These interactions provide new avenues for effective air quality regulations and emphasize the need to consider multiple pollutants simultaneously.

■ ASSOCIATED CONTENT

Ⓢ Supporting Information

$PM_{2.5}$ component concentration maps, a detailed model-measurement comparison, further analysis of the SO_2 oxidation

pathways, and a comparison of a linear extrapolation to the full model. This material is available free of charge via the Internet at http://pubs.acs.org.

■ AUTHOR INFORMATION

Corresponding Author

*Phone: 617 253 6281. Fax: 617 258 7733. E-mail: jareth@mit. edu.

Notes

The authors declare no competing financial interest.

■ REFERENCES

(1) Pope, C. A. Review: Epidemiological Basis for Particulate Air Pollution Health Standards. *Aerosol Sci. Technol.* **2000**, *32*, 4−14.

(2) US Environmental Protection Agency. National Emissions Inventory (NEI) air pollutant emissions trends data. http://www.epa.gov/ttnchie1/trends/ (accessed Nov 24, 2014).

(3) Ansari, A. S.; Pandis, S. N. Response of Inorganic PM to Precursor Concentrations. *Environ. Sci. Technol.* **1998**, *32*, 2706−2714.

(4) Takahama, S.; Wittig, A. E.; Vayenas, D. V.; Davidson, C. I.; Pandis, S. N. Modeling the diurnal variation of nitrate during the Pittsburgh Air Quality Study. *J. Geophys. Res.* **2004**, *109*, No. D16S06.

(5) Pinder, R. W.; Adams, P. J.; Pandis, S. N. Ammonia Emission Controls as a Cost-Effective Strategy for Reducing Atmospheric Particulate Matter in the Eastern United States. *Environ. Sci. Technol.* **2007**, *41*, 380−386.

(6) Makar, P. A.; Moran, M. D.; Zheng, Q.; Cousineau, S.; Sassi, M.; Duhamel, A.; Besner, M.; Davignon, D.; Crevier, L.-P.; Bouchet, V. S. Modelling the impacts of ammonia emissions reductions on North American air quality. *Atmos. Chem. Phys.* **2009**, *9*, 7183−7212.

(7) Henze, D. K.; Seinfeld, J. H.; Shindell, D. T. Inverse modeling and mapping US air quality influences of inorganic PM₂.₅ precursor emissions using the adjoint of GEOS-Chem. *Atmos. Chem. Phys.* **2009**, *9*, 5877−5903.

(8) Paulot, F.; Jacob, D. J. Hidden Cost of U.S. Agricultural Exports: Particulate Matter from Ammonia Emissions. *Environ. Sci. Technol.* **2013**, *48*, 903−908.

(9) West, J.; Ansari, A.; Pandis, S. Marginal PM2.5: Nonlinear Aerosol Mass Response to Sulfate Reductions in the Eastern United States. *J. Air Waste Manage. Assoc.* **1999**, *49*, 1415−1424.

(10) Manktelow, P. T.; Mann, G. W.; Carslaw, K. S.; Spracklen, D. V.; Chipperfield, M. P. Regional and global trends in sulfate aerosol since the 1980s. *Geophys. Res. Lett.* **2007**, *34*, No. L14803.

(11) Leibensperger, E. M.; Mickley, L. J.; Jacob, D. J.; Barrett, S. R. H. Intercontinental influence of NOx and CO emissions on particulate matter air quality. *Atmos. Environ.* **2011**, *45*, 3318−3324.

(12) Muller, N. Z.; Mendelsohn, R. Measuring the damages of air pollution in the United States. *J. Environ. Econ. Manage.* **2007**, *54*, 1−14.

(13) Caiazzo, F.; Ashok, A.; Waitz, I. A.; Yim, S. H. L.; Barrett, S. R. H. Air pollution and early deaths in the United States. Part I: Quantifying the impact of major sectors in 2005. *Atmos. Environ.* **2013**, *79*, 198−208.

(14) Hakami, A.; Odman, M. T.; Russell, A. G. High-Order, Direct Sensitivity Analysis of Multidimensional Air Quality Models. *Environ. Sci. Technol.* **2003**, *37*, 2442−2452.

(15) Hakami, A. Nonlinearity in atmospheric response: A direct sensitivity analysis approach. *J. Geophys. Res.* **2004**, *109*, No. D15303.

(16) Wagstrom, K. M.; Pandis, S. N.; Yarwood, G.; Wilson, G. M.; Morris, R. E. Development and application of a computationally efficient particulate matter apportionment algorithm in a three-dimensional chemical transport model. *Atmos. Environ.* **2008**, *42*, 5650−5659.

(17) Zhang, W.; Capps, S. L.; Hu, Y.; Nenes, A.; Napelenok, S. L.; Russell, A. G. Development of the high-order decoupled direct method in three dimensions for particulate matter: enabling advanced sensitivity analysis in air quality models. *Geosci. Model Dev.* **2012**, *5*, 355−368.

(18) Hakami, A.; Henze, D. K.; Seinfeld, J. H.; Singh, K.; Sandu, A.; Kim, S.; Li, Q. The Adjoint of CMAQ. *Environ. Sci. Technol.* **2007**, *41*, 7807−7817.

(19) Henze, D. K.; Hakami, A.; Seinfeld, J. H. Development of the adjoint of GEOS-Chem. *Atmos. Chem. Phys.* **2007**, *7*, 2413−2433.

(20) Muller, N. Z.; Mendelsohn, R.; Nordhaus, W. Environmental accounting for pollution in the United States economy. *Am. Econ. Rev.* **2011**, *101*, 1649−1675.

(21) Muller, N. Z. Linking Policy to Statistical Uncertainty in Air Pollution Damages Linking Policy to Statistical Uncertainty in Air Pollution Damages. *B. E. J. Econ. Anal. Policy* **2011**, *11*, No. 32.

(22) Fann, N.; Baker, K. R.; Fulcher, C. M. Characterizing the PM₂.₅-related health benefits of emission reductions for 17 industrial, area and mobile emission sectors across the U.S. *Environ. Int.* **2012**, *49*, 141−151.

(23) Fann, N.; Fulcher, C. M.; Baker, K. The recent and future health burden of air pollution apportioned across U.S. sectors. *Environ. Sci. Technol.* **2013**, *47*, 3580−3589.

(24) Fann, N.; Fulcher, C. M.; Hubbell, B. J. The influence of location, source, and emission type in estimates of the human health benefits of reducing a ton of air pollution. *Air Qual. Atmos. Health* **2009**, *2*, 169−176.

(25) *Technical Support Document for the Proposed PM NAAQS Rule*; US Environmental Protection Agency, Office of Air Quality Planning and Standards: Research Triangle Park, NC, 2006.

(26) Bey, I.; Jacob, D. J.; Yantosca, R. M.; Logan, J. A.; Field, B. D.; Fiore, A. M.; Li, Q.; Liu, H. Y.; Mickley, L. J.; Schultz, M. G. Global modeling of tropospheric chemistry with assimilated meteorology: Model description and evaluation. *J. Geophys. Res.* **2001**, *106*, 23073−23095.

(27) Park, R. J.; Jacob, D. J.; Field, B. D.; Yantosca, R. M.; Chin, M. Natural and transboundary pollution influences on sulfate-nitrate-ammonium aerosols in the United States: Implications for policy. *J. Geophys. Res. Atmos* **2004**, *109*, No. D15204.

(28) Walker, J. M.; Philip, S.; Martin, R. V.; Seinfeld, J. H. Simulation of nitrate, sulfate, and ammonium aerosols over the United States. *Atmos. Chem. Phys.* **2012**, *12*, 11213−11227.

(29) Heald, C. L.; Collett, J. L. J.; Lee, T.; Benedict, K. B.; Schwandner, F. M.; Li, Y.; Clarisse, L.; Hurtmans, D. R.; Van Damme, M.; Clerbaux, C.; et al. Atmospheric ammonia and particulate inorganic nitrogen over the United States. *Atmos. Chem. Phys.* **2012**, *12*, 10295−10312.

(30) Pye, H. O. T.; Liao, H.; Wu, S.; Mickley, L. J.; Jacob, D. J.; Henze, D. K.; Seinfeld, J. H. Effect of changes in climate and emissions on future sulfate-nitrate-ammonium aerosol levels in the United States. *J. Geophys. Res. Atmos* **2009**, *114*, No. D01205.

(31) Leibensperger, E. M.; Mickley, L. J.; Jacob, D. J.; Chen, W.-T.; Seinfeld, J. H.; Nenes, A.; Adams, P. J.; Streets, D. G.; Kumar, N.; Rind, D. Climatic effects of 1950−2050 changes in US anthropogenic aerosols − Part 2: Climate response. *Atmos. Chem. Phys.* **2012**, *12*, 3349−3362.

(32) Leibensperger, E. M.; Mickley, L. J.; Jacob, D. J.; Chen, W.-T.; Seinfeld, J. H.; Nenes, A.; Adams, P. J.; Streets, D. G.; Kumar, N.; Rind, D. Climatic effects of 1950−2050 changes in US anthropogenic aerosols − Part 1: Aerosol trends and radiative forcing. *Atmos. Chem. Phys.* **2012**, *12*, 3333−3348.

(33) Fountoukis, C.; Nenes, A. ISORROPIA II: a computationally efficient thermodynamic equilibrium model for K⁺−Ca²⁺−Mg²⁺−NH₄⁺−Na⁺−SO₄²⁻−NO₃⁻−Cl⁻−H₂O aerosols. *Atmos. Chem. Phys.* **2007**, *7*, 4639−4659.

(34) Wang, Y. X. A nested grid formulation for chemical transport over Asia: Applications to CO. *J. Geophys. Res.* **2004**, *109*, No. D22307.

(35) Zhang, Y.; Jaeglé, L.; van Donkelaar, A.; Martin, R. V.; Holmes, C. D.; Amos, H. M.; Wang, Q.; Talbot, R.; Artz, R.; Brooks, S.; et al.

Nested-grid simulation of mercury over North America. *Atmos. Chem. Phys.* **2012**, *12*, 6095−6111.

(36) Hudman, R. C.; Moore, N. E.; Martin, R. V.; Russell, A. R.; Mebust, A. K.; Valin, L. C.; Cohen, R. C. A mechanistic model of global soil nitric oxide emissions: implementation and space based-constraints. *Atmos. Chem. Phys. Discuss.* **2012**, *12*, 3555−3594.

(37) Liu, S.; Liang, X.-Z. Observed Diurnal Cycle Climatology of Planetary Boundary Layer Height. *J. Clim.* **2010**, *23*, 5790−5809.

(38) Zhang, L.; Jacob, D. J.; Knipping, E. M.; Kumar, N.; Munger, J. W.; Carouge, C. C.; van Donkelaar, A.; Wang, Y. X.; Chen, D. Nitrogen deposition to the United States: distribution, sources, and processes. *Atmos. Chem. Phys.* **2012**, *12*, 4539−4554.

(39) Macintyre, H. L.; Evans, M. J. Sensitivity of a global model to the uptake of N_2O_5 by tropospheric aerosol. *Atmos. Chem. Phys.* **2010**, *10*, 7409−7414.

(40) Van Donkelaar, A.; Martin, R. V.; Leaitch, W. R.; Macdonald, A. M.; Walker, T. W.; Streets, D. G.; Zhang, Q.; Dunlea, E. J.; Jimenez, J. L.; Dibb, J. E.; et al. Analysis of aircraft and satellite measurements from the Intercontinental Chemical Transport Experiment (INTEX-B) to quantify long-range transport of East Asian sulfur to Canada. *Atmos. Chem. Phys.* **2008**, *8*, 2999−3014.

(41) Pinder, R. W.; Adams, P. J.; Pandis, S. N.; Gilliland, A. B. Temporally resolved ammonia emission inventories: Current estimates, evaluation tools, and measurement needs. *J. Geophys. Res. Atmos* **2006**, *111*, No. D16310.

(42) Tong, D. Q.; Lamsal, L.; Pan, L.; Ding, C.; Kim, H.; Lee, P.; Chai, T.; Pickering, K. E.; Stajner, I. Long-term NOx trends over large cities in the United States during the great recession: Comparison of satellite retrievals, ground observations, and emission inventories. *Atmos. Environ.* **2015**, *107*, 70−84.

(43) Duncan, B. N.; Yoshida, Y.; de Foy, B.; Lamsal, L. N.; Streets, D. G.; Lu, Z.; Pickering, K. E.; Krotkov, N. A. The observed response of Ozone Monitoring Instrument (OMI) NO_2 columns to NOx emission controls on power plants in the United States: 2005−2011. *Atmos. Environ.* **2013**, *81*, 102−111.

(44) Russell, A. R.; Valin, L. C.; Cohen, R. C. Trends in OMI NO_2 observations over the United States: effects of emission control technology and the economic recession. *Atmos. Chem. Phys.* **2012**, *12*, 12197−12209.

(45) Fioletov, V. E.; McLinden, C. A.; Krotkov, N.; Moran, M. D.; Yang, K. Estimation of SO_2 emissions using OMI retrievals. *Geophys. Res. Lett.* **2011**, *38*, No. L21811.

(46) Malm, W. C.; Sisler, J. F.; Huffman, D.; Eldred, R. A.; Cahill, T. A. Spatial and seasonal trends in particle concentration and optical extinction in the United States. *J. Geophys. Res.* **1994**, *99*, 1347.

(47) US Environmental Protection Agency. Daily summary data for particulates. http://aqsdr1.epa.gov/aqsweb/aqstmp/airdata/download_files.html#Daily (accessed Nov 24, 2014).

(48) Simon, H.; Baker, K. R.; Phillips, S. Compilation and interpretation of photochemical model performance statistics published between 2006 and 2012. *Atmos. Environ.* **2012**, *61*, 124−139.

(49) Seinfeld, J. H.; Pandis, S. N.*Atmospheric Chemistry and Physics: From Air Pollution to Climate Change*; John Wiley & Sons: New York, 2012; p 1203.

(50) Duncan, B. N.; Yoshida, Y.; Olson, J. R.; Sillman, S.; Martin, R. V.; Lamsal, L.; Hu, Y.; Pickering, K. E.; Retscher, C.; Allen, D. J.; et al. Application of OMI observations to a space-based indicator of NOx and VOC controls on surface ozone formation. *Atmos. Environ.* **2010**, *44*, 2213−2223.

(51) Pakkanen, T. A.; Hillamo, R. E.; Aurela, M.; Andersen, H. V.; Grundahl, L.; Ferm, M.; Persson, K.; Karlsson, V.; Reissell, A.; Røyset, O.; et al. Nordic intercomparison for measurement of major atmospheric nitrogen species. *J. Aerosol Sci.* **1999**, *30*, 247−263.

(52) Schaap, M.; Spindler, G.; Schulz, M.; Acker, K.; Maenhaut, W.; Berner, A.; Wieprecht, W.; Streit, N.; Müller, K.; Brüggemann, E.; et al. Artefacts in the sampling of nitrate studied in the "INTERCOMP" campaigns of EUROTRAC-AEROSOL. *Atmos. Environ.* **2004**, *38*, 6487−6496.

(53) Kant Pathak, R.; Chan, C. K. Inter-particle and gas-particle interactions in sampling artifacts of PM in filter-based samplers. *Atmos. Environ.* **2005**, *39*, 1597−1607.

(54) Squizzato, S.; Masiol, M.; Brunelli, A.; Pistollato, S.; Tarabotti, E.; Rampazzo, G.; Pavoni, B. Factors determining the formation of secondary inorganic aerosol: a case study in the Po Valley (Italy). *Atmos. Chem. Phys.* **2013**, *13*, 1927−1939.

(55) Pinder, R. W.; Dennis, R. L.; Bhave, P. V. Observable indicators of the sensitivity of PM2.5 nitrate to emission reductions—Part I: Derivation of the adjusted gas ratio and applicability at regulatory-relevant time scales. *Atmos. Environ.* **2008**, *42*, 1275−1286.

(56) Dennis, R. L.; Bhave, P. V.; Pinder, R. W. Observable indicators of the sensitivity of PM2.5 nitrate to emission reductions—Part II: Sensitivity to errors in total ammonia and total nitrate of the CMAQ-predicted non-linear effect of SO_2 emission reductions. *Atmos. Environ.* **2008**, *42*, 1287−1300.

(57) Bertram, T. H.; Thornton, J. A.; Riedel, T. P.; Middlebrook, A. M.; Bahreini, R.; Bates, T. S.; Quinn, P. K.; Coffman, D. J. Direct observations of N2O5 reactivity on ambient aerosol particles. *Geophys. Res. Lett.* **2009**, *36*, No. L19803.

(58) Wen, L.; Chen, J.; Yang, L.; Wang, X.; Sui, X.; Yao, L.; Zhu, Y.; Zhang, J.; Zhu, T.; Wang, W. Enhanced formation of fine particulate nitrate at a rural site on the North China Plain in summer: the important roles of ammonia and ozone. *Atmos. Environ.* **2014**, *101*, 294−302.

(59) Chang, W. L.; Bhave, P. V.; Brown, S. S.; Riemer, N.; Stutz, J.; Dabdub, D. Heterogeneous Atmospheric Chemistry, Ambient Measurements, and Model Calculations of N_2O_5: A Review. *Aerosol Sci. Technol.* **2011**, *45*, 665−695.

(60) Simon, H.; Kimura, Y.; McGaughey, G.; Allen, D. T.; Brown, S. S.; Coffman, D.; Dibb, J.; Osthoff, H. D.; Quinn, P.; Roberts, J. M. Modeling heterogeneous $ClNO_2$ formation, chloride availability, and chlorine cycling in Southeast Texas. *Atmos. Environ.* **2010**, *44*, 5476−5488.

(61) Hudson, P. K.; Schwarz, J.; Baltrusaitis, J.; Gibson, E. R.; Grassian, V. H. A spectroscopic study of atmospherically relevant concentrated aqueous nitrate solutions. *J. Phys. Chem. A* **2007**, *111*, 544−548.

(62) Archibald, A. T.; Jenkin, M. E.; Shallcross, D. E. An isoprene mechanism intercomparison. *Atmos. Environ.* **2010**, *44*, 5356−5364.

(63) Li, Y.; Henze, D. K.; Jack, D.; Kinney, P. L. The influence of air quality model resolution on health impact assessment for fine particulate matter and its components. *Air Qual., Atmos. Health* **2015**, DOI: 10.1007/s11869-015-0321-z.

(64) Thompson, T. M.; Saari, R. K.; Selin, N. E. Air quality resolution for health impact assessment: influence of regional characteristics. *Atmos. Chem. Phys.* **2014**, *14*, 969−978.

(65) Punger, E. M.; West, J. J. The effect of grid resolution on estimates of the burden of ozone and fine particulate matter on premature mortality in the United States. *Air Qual., Atmos. Health* **2013**, *6*, 563−573.

MIT Joint Program on the Science and Policy of Global Change - REPRINT SERIES

2014-13   Water Consumption Footprint and Land Requirements of Large-Scale Alternative Diesel and Jet Fuel Production, Staples, M.D., H. Olcay, R. Malina, P. Trivedi, M.N. Pearlson, K. Strzepek, S.V. Paltsev, C. Wollersheim and S.R.H. Barrett, *Environmental Science & Technology*, 47: 12557–12565 (2013)

2014-14   The Potential Wind Power Resource in Australia: A New Perspective, Hallgren, W., U.B. Gunturu and A. Schlosser, *PLoS ONE,* 9(7): e99608, doi: 10.1371/journal.pone.0099608 (2014)

2014-15   Trend analysis from 1970 to 2008 and model evaluation of EDGARv4 global gridded anthropogenic mercury emissions, Muntean, M., G. Janssens-Maenhout, S. Song, N.E. Selin, J.G.J. Olivier, D. Guizzardi, R. Maas and F. Dentener, *Science of the Total Environment,* 494-495(2014): 337-350 (2014)

2014-16   The future of global water stress: An integrated assessment, Schlosser, C.A., K. Strzepek, X. Gao, C. Fant, É. Blanc, S. Paltsev, H. Jacoby, J. Reilly and A. Gueneau, *Earth's Future,* 2, online first (doi: 10.1002/2014EF000238) (2014)

2014-17   Modeling U.S. water resources under climate change, Blanc, É., K. Strzepek, A. Schlosser, H. Jacoby, A. Gueneau, C. Fant, S. Rausch and J. Reilly, *Earth's Future,* 2(4): 197–244 (doi: 10.1002/2013EF000214) (2014)

2014-18   Compact organizational space and technological catch-up: Comparison of China's three leading automotive groups, Nam, K.-M., *Research Policy*, online first (doi: 10.1002/2013EF000214) (2014)

2014-19   Synergy between pollution and carbon emissions control: Comparing China and the United States, Nam, K.-M., C.J. Waugh, S. Paltsev, J.M. Reilly and V.J. Karplus, *Energy Economics*, 46(November): 186–201 (2014)

2014-20   The ocean's role in the transient response of climate to abrupt greenhouse gas forcing, Marshall, J., J.R. Scott, K.C. Armour, J.-M. Campin, M. Kelley and A. Romanou, *Climate Dynamics*, online first (doi: 10.1007/s00382-014-2308-0) (2014)

2014-21   The ocean's role in polar climate change: asymmetric Arctic and Antarctic responses to greenhouse gas and ozone forcing, Marshall, J., K.C. Armour, J.R. Scott, Y. Kostov, U. Hausmann, D. Ferreira, T.G. Shepherd and C.M. Bitz, *Philosophical Transactions of the Royal Society A*, 372: 20130040 (2014).

2014-22   Emissions trading in China: Progress and prospects, Zhang, D., V.J. Karplus, C. Cassisa and X. Zhang, *Energy Policy,* 75(December): 9–16 (2014)

2014-23   The mercury game: evaluating a negotiation simulation that teaches students about science-policy interactions, Stokes, L.C. and N.E. Selin, *Journal of Environmental Studies & Sciences*, online first (doi:10.1007/s13412-014-0183-y) (2014)

2014-24   Climate Change and Economic Growth Prospects for Malawi: An Uncertainty Approach, Arndt, C., C.A. Schlosser, K.Strzepek and J. Thurlow, J*ournal of African Economies,* 23(Suppl 2): ii83–ii107 (2014)

2014-25   Antarctic ice sheet fertilises the Southern Ocean, Death, R., J.L.Wadham, F. Monteiro, A.M. Le Brocq, M. Tranter, A. Ridgwell, S. Dutkiewicz and R. Raiswell, *Biogeosciences*, 11, 2635–2644 (2014)

2014-26   Understanding predicted shifts in diazotroph biogeography using resource competition theory, Dutkiewicz, S., B.A. Ward, J.R. Scott and M.J. Follows, *Biogeosciences,* 11, 5445–5461 (2014)

2**2014-27   Coupling the high-complexity land surface model ACASA to the mesoscale model WRF,** L. Xu, R.D. Pyles, K.T. Paw U, S.H. Chen and E. Monier, *Geoscientific Model Development*, 7, 2917–2932 (2014)

2015-1   Double Impact: Why China Needs Separate But Coordinated Air Pollution and CO$_2$ Reduction Strategies, Karplus, V.J., *Paulson Papers on Energy and Environment* (2015)

2015-2   Behavior of the aggregate wind resource in the ISO regions in the United States, Gunturu, U.B. and C.A. Schlosser, *Applied Energy*, 144(April): 175–181 (2015)

2015-3   Analysis of coastal protection under rising flood risk, Lickley, M.J., N. Lin and H.D. Jacoby, *Climate Risk Management*, 6(2014): 18–26 (2015)

2015-4   Benefits of greenhouse gas mitigation on the supply, management, and use of water resources in the United States, K. Strzepek et al., *Climatic Change,* online first (doi: 10.1007/s10584-014-1279-9) (2015)

2015-5   Modeling Regional Transportation Demand in China and the Impacts of a National Carbon Policy, Kishimoto, P.N., D. Zhang, X. Zhang and V.J. Karplus, *Transportation Research Record* 2454: 1-11 (2015)

2015-6   Impacts of the Minamata Convention on Mercury Emissions and Global Deposition from Coal-Fired Power Generation in Asia, Giang, A., L.C. Stokes, D.G. Streets, E.S. Corbitt and N.E. Selin, *Environmental Science & Technology,* online first (doi: 10.1021/acs.est.5b00074) (2015)

2015-7   Climate change policy in Brazil and Mexico: Results from the MIT EPPA model, Octaviano, C., S. Paltsev and A. Gurgel, *Energy Economics*, online first (doi: 10.1016/j. eneco.2015.04.007) (2015)

2015-8   Changes in Inorganic Fine Particulate Matter Sensitivities to Precursors Due to Large-Scale US Emissions Reductions, Holt, J., N.E. Selin and S. Solomon, *Environmental Science & Technology*, 49(8): 4834–4841 (2015)